LiDAR Uncertainty Quantification for Topo-Bathymetric Earth Science using Generalized Polynomial Chaos Expansion

GC15A-49

Alexandra K. Wise[1], Kevin W. Sacca[1], Jeffrey P. Thayer[1]*

[1] Aerospace Engineering Sciences Department, University of Colorado Boulder

***Corresponding Author: Alexandra.Wise@Colorado.edu**

Motivation and Overview

Motivation: Most LiDARs are vulnerable to position, pointing errors, and propagation effects leading to projection errors on target. While fidelity of location/ pointing solutions can be high, determination of uncertainty remains limited. NASA's 2021 STV Incubation Study Report lists vertical (horizontal, geolocation) accuracy as an associated product parameter for all (most) identified Science and Application Knowledge Gaps.

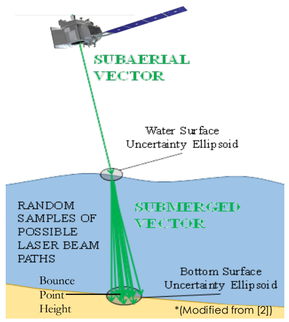

gPCE Method Overview:

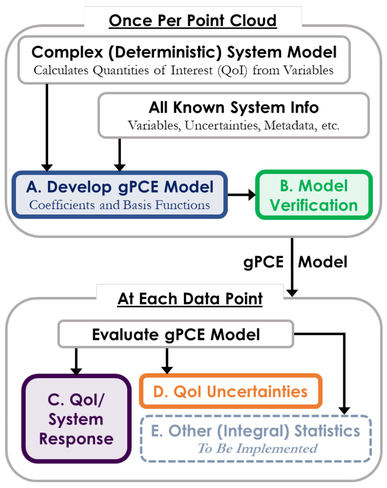

Research Objectives:

- Develop gPCE method for topo-bathymetric LiDAR Uncertainty Quantification (UQ) as an alternative to Total Propagated Uncertainty & Monte Carlo UQ methods
- Quantify & compare performance of UQ methods, in terms of computational cost & model fidelity
- Investigate subaerial simulations as validation to proceed with bathymetric simulation (topographic/bare-earth results presented here; bathymetric results forthcoming)

A. generalized Polynomial Chaos Expansion (gPCE) Modeling

$$\begin{bmatrix} y_1 \\ y_2 \\ \vdots \\ y_N \end{bmatrix} \Rightarrow \text{Complex (Deterministic) System/Algorithm} \Rightarrow \begin{bmatrix} u(y_1) \\ u(y_2) \\ \vdots \\ u(y_N) \end{bmatrix} \Rightarrow \begin{bmatrix} \Psi_0(y_1) & \cdots & \Psi_P(y_1) \\ \vdots & \ddots & \vdots \\ \Psi_0(y_N) & \cdots & \Psi_P(y_N) \end{bmatrix} \begin{bmatrix} c_0 \\ \vdots \\ c_P \end{bmatrix} \approx \begin{bmatrix} u(y_1) \\ \vdots \\ u(y_N) \end{bmatrix}$$

Generate Input Samples — Generate Solution Samples — Construct & Invert to Find c_i

$$\Rightarrow \hat{u}(y) \approx \sum_{i=0}^{P} c_i \Psi_{j_i}(y) \Rightarrow \textit{Quick and High Fidelity Computation of Complex Phenomena}$$

gPCE Model

$$(\Psi_{j_i}(y) = \psi_{j_{(i,1)}}(y_1) * \cdots * \psi_{j_{(i,d)}}(y_d))$$

y	Distribution of y	Askey Polynomial	Support
Continuous	Gaussian	Hermite	$(-\infty, +\infty)$
	Gamma	Laguerre	$(0, +\infty)$
	Beta	Jacobi	$[a, b]$
	Uniform	Legendre	$[a, b]$
Discrete	Poisson	Charlier	$\{0, 1, \cdots\}$
	Binomial	Krawtchouk	$\{0, 1 \cdots, N\}$

W. Schoutens, 2000, D. Xiu and G. Karniadakis, 2002

A.1) generalized Polynomial Chaos Expansion analogous to Fourier Expansions

- Truncated infinite series of coefficients & orthogonal basis functions (Karhunen-Loève Expansion)
- Multi-variate Askey basis functions used → minimized mean squared error and guaranteed convergence

A.2) General gPCE model finding procedure (see above)

- Solution samples, $\boldsymbol{u}(\boldsymbol{y_i})$, generated using ICESat-2 photon bounce point location algorithm analog
- Multi-variate basis functions, $\boldsymbol{\Psi_{j_i}(y_i)}$, evaluated at inputs, $\boldsymbol{y_i}$, basis function matrix, $\bar{\boldsymbol{\Psi}}$, constructed
- $\bar{\boldsymbol{\Psi}}\boldsymbol{c} = \boldsymbol{u}$ inverted to solve for gPCE coefficients, $\boldsymbol{c}$
  - L2 Minimization (Ordinary Least Squares) currently used for inversion
  - Sparse matrix inversion methods to be implemented for better convergence

A.3) Using gPCE Models and Calculating Uncertainties

- Quantities of Interest (QoI), e.g., photon bounce point location, calculated directly from inputs
- QoI uncertainties calculated by integrating input variable uncertainties near input variable values
  - Inputs, $\boldsymbol{y_i}$, are intrinsically treated as stochastic by default by the gPCE method
  - Inputs modeled as $y_i = x_i + \omega_i$, with deterministic input, x, and (stochastic) input uncertainty, ω
- Uncertainties determined "At Each Data Point," with low individual computational cost
  - Only single-variate basis functions (in ω_i) require integration to compute uncertainty
  - Can be pre-computed because of separable inputs
- Coefficient selection optimizes computational cost, while managing model fidelity

B. gPCE Lidar Model Verification, Model Error

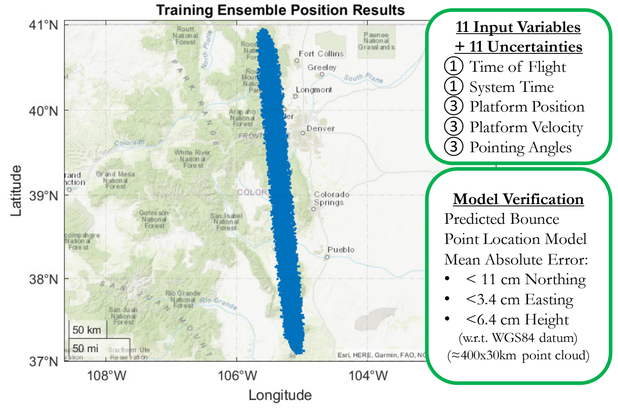

11 Input Variables + 11 Uncertainties

- (1) Time of Flight
- (1) System Time
- (3) Platform Position
- (3) Platform Velocity
- (3) Pointing Angles

Model Verification

Predicted Bounce Point Location Model Mean Absolute Error:

- < 11 cm Northing
- <3.4 cm Easting
- <6.4 cm Height

(w.r.t. WGS84 datum) (≈400x30km point cloud)

Histograms of Error in Verification Points

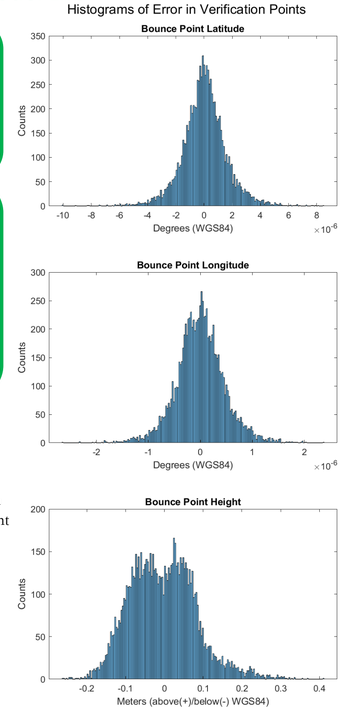

B.1) gPCE can be applied to diverse platforms and concepts of operation to rapidly assess measurement domains, systems, and techniques

- Space-based ICESAT-2/ATLAS LiDAR's subaerial path serves as model algorithm test case → Subaqueous, satellite- (and drone-) based algorithms under development

B.2) High-fidelity gPCE model created using ICESAT-2/ATLAS photon bounce point geolocation algorithm analog

- Large variable range of the 11 input parameters used to train model → Allows model to accurately represent a large range of operational conditions

B.3) Minimizing model errors enhances model predictive power

- Model Verification success criterion met, when model error << science requirements on error

C. ICESat-2/ATLAS gPCE Model System Response & D. gPCE Model Uncertainty Quantification

C.1) gPCE enables high fidelity, simultaneous assessment of parameter relationships

- Input variables (11, in this case, plus 11 uncertainties) form hyper-plane of multi-variate system relationships
- 2-Input response surfaces displayed to best visualize input-output variable effects
- Topographic results presented for simplicity; bathymetric bounce point location algorithm in development
- Valid, highly sparse gPC expansion found
  - <13 terms (of 2300) in each variable have a relative significance >1%
  - >40% of expansion terms can be discarded with negligible change in error
- Simultaneous, computationally efficient, calculation of quantities of interest and uncertainty supported by gPCE

C.2) gPCE model reveals non-intuitive system response characteristics

- Significant non-intuitive behavior can be revealed in high-correlation relationships
- Yaw angle of near-nadir pointed lidar system caused significant effect, ignoring this contribution could have result in up to 6 cm of error (see figure below)

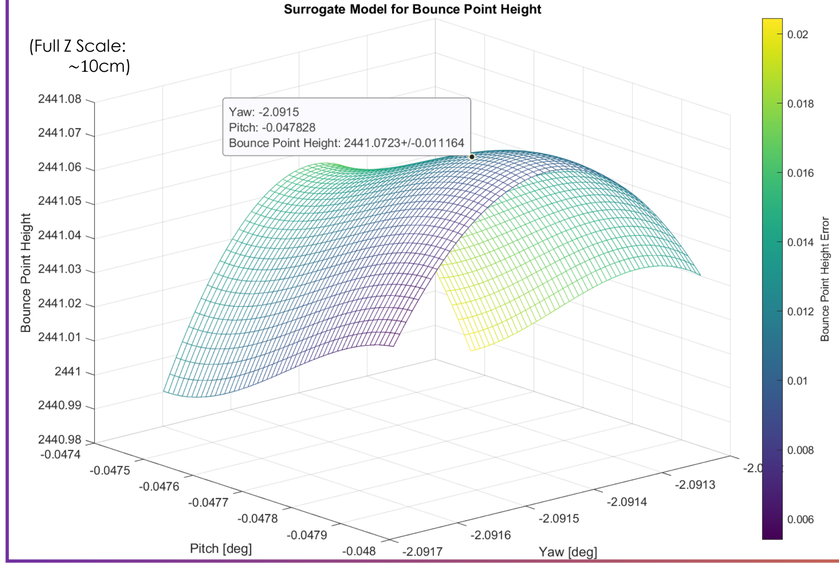

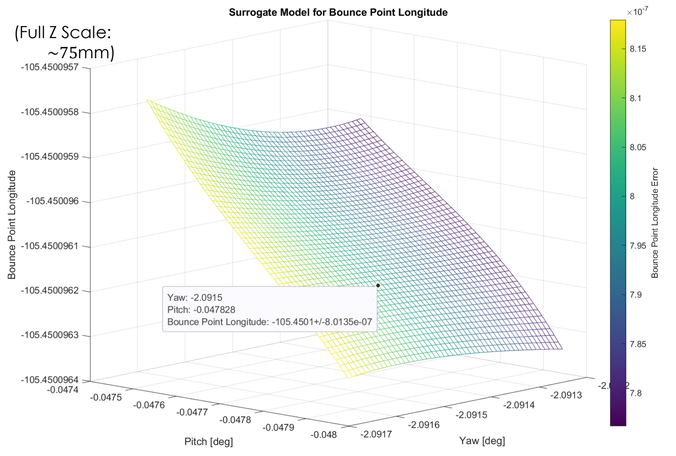

D.1) gPCE makes minimal *a priori* assumptions, seeks to fit model to best available information

- Traditional error analysis methods may miss significant relationships due to simplifying assumptions, e.g., all errors Gaussian and uncorrelated (or low correlation), or through unmodeled physics (excluded variables) in error analyses, or assuming negligible impact of certain variables on overall final error

D.2) Real variable relationships likely to be correlated

- Errors may, or may not, be properly represented by traditional techniques, especially if degree of correlation is low, but non-zero (see figure above), or if a single variable dominates the relationship
- gPCE captures nonlinearities often ignored by traditional UQ techniques

Variables used in this simulation are from ICESat-2 ATL02, ATL03 data, and span the Region 2 granule. Surrogate Model Graph corresponds to a specific LiDAR bounce point in the mountains west of Boulder, CO, at ~40.0N, 105.4W. (NOTE: The authors recognize that Pitch, Yaw do not represent real ATLAS pointing angles; in the interest of model simplicity, Pitch, Roll, Yaw, were varied as a substitute for real pointing data, with other pointing variables held fixed.)

Future Research

1) Automate Coefficient Thresholding and Point Error Ellipsoid Computation

- Current codebase only allows for manual coefficient thresholding and point error ellipsoid computation, automatic procedures necessary for successful deployment of code to actual lidar applications
- Enables "simulated error" truth-testing for model self-verification and validation

2) Optimize Sparsity of Coefficient Matrix

- Computationally optimal solution is a sparse solution of large coefficients
- Improved coefficient inversion solvers (such as those utilizing L1 minimization methods) needed to decrease computational complexity (convex, P-time vs. non-convex, NP-hard problems)

3) Advance Towards a Bathymetric LiDAR model

- Verify topographic model computational stability and cost
- Characterize bathymetric impact on geolocation algorithm
- Use point cloud gPCE model & UQ estimates for underwater object classification

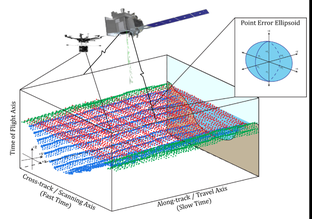

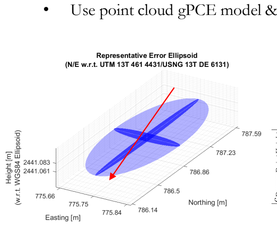

(Northing axis not to scale.

Approximate flight path angle in red.)

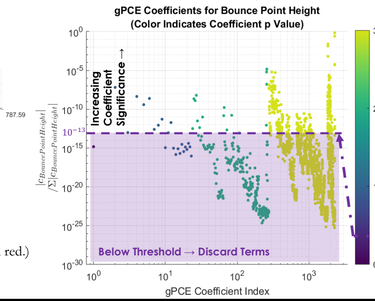

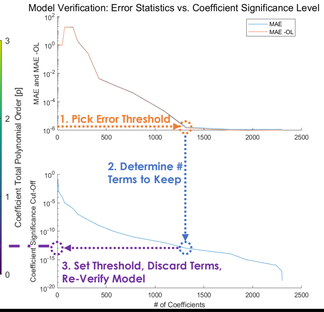

Acknowledgements

The Authors would like to thank Professor Alireza Doostan, for his assistance in applying the gPCE Method to Air- and Spaceborne Topo-Bathymetric LiDAR Measurements, and the NASA FINESST and USACE/DOD Strategic Environmental Restoration Development (SERDP) programs for funding support.

Funding :

- NASA FINESST Award #80NSSC19K1351
- NASA FINESST Award #80NSSC21K1597
- SERDP Contract #W912HQ22C0042

References

[1] S. B. Luthcke, T. C. Thomas, T. A. Pennington, T. W. Rebold, J. B. Nicholas, D. D. Rowlands, A. S. Gardner, and S. Bae, "ICESat-2 Pointing Calibration and Geolocation Performance," Earth and Space Science, vol. 8, no. 3, pp. 1–11, 2021.

[2] F. Eren, J. Jung, C. E. Parrish, N. Sarkozi-Forfinski, and B. R. Calder, "Total vertical uncertainty (TVU) modeling for topo-bathymetric LIDAR systems," Photogrammetric Engineering and Remote Sensing, vol. 85, no. 8, pp. 585–596, 2019.

[3] T. R. Scott B. Luthcke, Teresa Pennington and T. Thomas, "ICESat-2 ATL03g: ATBD for ATL03g ICESat-2 Receive Photon Geolocation," tech. rep., 2019.

[4] S. Bae, L. Magruder, N. Smith, and B. Schutz, "ICESat-2 ATBD for Precision Pointing Determination," tech. rep.

[5] A. J. Martino, M. R. Bock, T. A. Neumann, D. W. H. Iii, R. L. J. Iii, P. W. Dabney, and C. E. Webb, "ICESat-2 ATL02: Level 1B Data Product Processing," tech. rep., 2020.

[6] T. Neumann, A. C. Brenner, D. W. Hancock, J. Robbins, J. Saba, K. Harbeck, and A. Gibbons, "ICESat-2 ATL03: ATBD for Global Geolocated Photons," tech. rep., 2019.

[7] S. Bae, B. Helgeson, M. James, L. Magruder, J. Sipps, S. Luthcke, and T. Thomas, "Performance of ICESat-2 Precision Pointing Determination," Earth and Space Science, vol. 8, no. 4, pp. 1–8, 2021.

[8] NATIONAL GEOSPATIAL-INTELLIGENCE AGENCY, "World Geodetic System 1984 (WGS84)," tech. rep., 2014.

[9] L. Petrov, "ICESat-2 ATL03a: ATBD for Atmospheric Delay Correction to Laser Altimetry Ranges," tech. rep., 2014.

[10] V. Coppola, J. H. Seago, and D. A. Vallado, "The IAU 2000A and IAU 2006 precession-nutation theories and their implementation," Advances in the Astronautical Sciences, vol. 134, no. January, pp. 919–938, 2009.

[11] S. B. Luthcke, N. P. Zelensky, D. D. Rowlands, F. G. Lemoine, and T. A. Williams, "The 1-centimeter orbit: Jason-1 precision orbit determination using GPS, SLR, DORIS, and altimeter data," Marine Geodesy, vol. 26, no. 3-4, pp. 399–421, 2003.

[12] S. B. Luthcke, T. Pennington, B. D. Loomis, T. Rebold, T. C. Thomas, and E. N. Gsfc, "ICESat-2 ATBD for Precise Orbit Determination, Orbit Design, and Geolocation Parameter Calibration," tech. rep., 2019.

[13] T. A. Neumann, A. Brenner, D. Hancock, J. Robbins, J. Saba, K. Harbeck, A. Gibbons, J. Lee, S. B. Luthcke, T. Rebold, and E. Al., "ICESat-2 ATL03 Known Issues," Tech. Rep. January 2021, NASA, 2021.